Bandwidth Allocation in Wireless ATM Networks with Guaranteed Cell Loss Performance*

Jeong Geun Kim and Marwan Krunz

Department of Electrical and Computer Engineering
University of Arizona
Tucson, AZ 85721
{jkkim, krunz}@ece.arizona.edu

Abstract

Wireless ATM aims at extending ATM services to the wireless environment. In contrast to wireline ATM, which is primarily based on reliable fiber optic, wireless ATM will have to cope with an unreliable radio channel. This poses a host of technical challenges related to the provisioning of quality of service (QoS) over a wireless link. Key issues include incorporating the characteristics of the wireless channel in the provisioning of the cell-level QoS, and improving the transport performance using error control mechanisms. In this paper, we analyze the cell loss performance over a wireless ATM link. We consider both cases of a single and multiplexed ATM connections. The link capacity fluctuates according to a fluid version of Gilbert-Elliot channel model. Traffic sources are modeled as on-off fluid processes. Our analytical framework incorporates the effects of error control schemes (i.e., ARQ and/or FEC), which are used to improve the transport performance over the wireless link. For the single-stream case, we derive the exact cell loss rate (CLR) due to buffer overflow at the sender side of the wireless link. We also obtain a closed-form approximation for the corresponding *wireless* effective bandwidth. In the case of multiplexed streams, we obtain a good approximation for the CLR using the Chernoff-Dominant Eigenvalue (CDE) approach. The expressions for the CLR and effective bandwidth are then used to study the optimal FEC code rate that guarantees the requested QoS while maximizing the utilization of the wireless bandwidth. Numerical results and simulations are used to verify the adequacy of our analysis and to study the impact of error control on the allocation of bandwidth for guaranteed cell loss performance.

keywords: Wireless ATM networks, QoS, effective bandwidth, fluid analysis.

*This research was supported by NSF through CAREER Award ANI-9733143. Part of this paper will be presented at the ACM/IEEE International Conference on Mobile Computing and Networking (MobiCom'98), Dallas, USA, October 1998.

1 Introduction

Wireless asynchronous transfer mode (ATM) is emerging as a potential transport solution for broadband wireless networks [1, 2, 21]. It aims at extending ATM services to the wireless environment. To achieve this goal, wireless ATM must support the quality-of-service (QoS) requirements associated with various ATM services. The provisioning of QoS is particularly difficult in the wireless environment due to the scarcity of bandwidth and to the high and fluctuating bit-error rates (BER) of the radio channel.

Conventional ATM traffic control and resource allocation strategies have been designed with the assumption that the underlying physical media are highly reliable. Since this assumption does not hold for wireless links, applying the same resource allocation strategies of wireline ATM to the wireless environment could result in poor performance [6]. For instance, in transporting TCP traffic over wireless ATM, TCP makes the implicit assumption that packet losses are caused by congestion, although such losses may in fact be caused by cell discarding due to channel errors [5, 6] (errored cells are discarded by the ATM Adaptation Layer, which sits under TCP). Eventually, TCP times out and invokes its congestion control mechanism, which unnecessarily reduces the throughput of the wireless channel.

The transport performance of a wireless ATM link can be improved by using error control schemes. Two classes of error control are commonly used in wireless communications: automatic repeat request (ARQ) and forward error correction (FEC) [6]. In general, ARQ is used to deliver data requiring higher reliability, whereas FEC is suitable for delay-sensitive traffic [6]. Recent studies suggest that hybrid ARQ/FEC might be more appropriate for a wireless ATM network [6, 17], particularly when the transported traffic streams exhibit diverse characteristics and QoS requirements. For instance, Available Bit Rate (ABR) connections with relaxed time constraints can use ARQ. In contrast, Constant Bit Rate (CBR) and Variable Bit Rate (VBR) connections that require low delay, jitter, and minimal cell loss may need a combination of FEC and ARQ with time-constrained retransmission [3].

In order to guarantee the requested QoS while maintaining an acceptable level of bandwidth utilization, ATM employs the concept of effective bandwidth in connection admission control (CAC) and service scheduling [8, 12]. Significant research has been done on the notion of effective bandwidth over wireline networks [7, 8, 11, 12, 15]. Guérin et al. proposed an approximate expression for the effective bandwidth of both individual and multiplexed connections, arguing that this approximation is necessary for real-time network traffic control [12]. Elwalid and Mitra studied the effective bandwidth for general Markovian traffic sources [8]. Elwalid et al. proposed an approximation for the cell loss rate (CLR) at an ATM multiplexer using a hybrid Chernoff-Dominant Eigenvalue (CDE) approach [9]. The research on effective bandwidth has generally been addressed in the context of high-speed (wired) ATM networks. Recently, Mohammadi et al. extended the concept of effective bandwidth to wireless ATM networks [19]. However, the impact of error control was not considered. Bandwidth allocation and FEC code optimization in wireless ATM networks were discussed in [24] using a simplified framework that did not involve traffic models and queuing analysis (traffic sources were characterized by their mean rates). The provisioning of guaranteed CLR was not investigated. In that study, the authors observed the existence of a tradeoff between FEC and the number of retransmitted cells.

In this work, we investigate the cell loss performance due to buffer overflow at the transmitter side of a wireless link. We consider two scenarios for transporting ATM traffic over a wireless link (Figure 1). In the first scenario, the wireless link is used to transport a single traffic stream. For example, in Figure 1 the terrestrial link between the mobile terminal (MT) and an access point (AP) is used to transport the traffic stream of Connection A. In the second scenario, multiple streams are multiplexed onto the same wireless link, which can be, for example, an intermediate satellite or microwave link. For both scenarios, we assume that the transmitter side of the wireless link maintains a finite-capacity cell buffer, which may occasionally overflow.

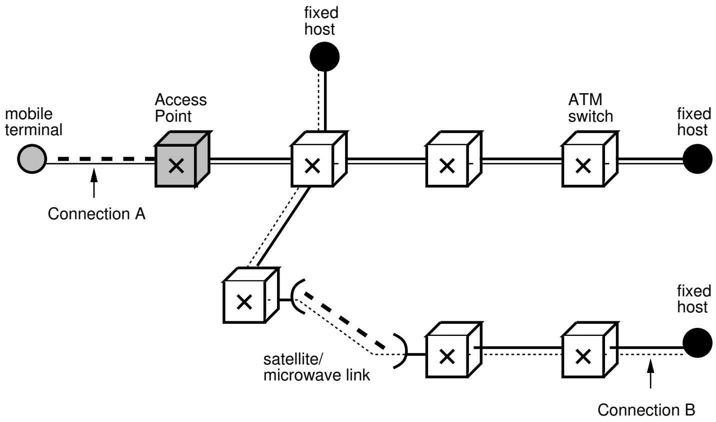

Figure 1: Two scenarios for transporting ATM traffic over a wireless link.

Cell losses are aggravated by the ARQ retransmission process, leading to a reduction in the effective service rate. Therefore, extra bandwidth must be assigned in order to compensate for the reduced service rate. This extra bandwidth can be assigned by increasing the service rate and/or the FEC rate. Increasing the service rate reduces the CLR although the quality of the wireless channel stays unchanged. In contrast, increasing the effectiveness of FEC improves the quality of the wireless channel at the expense of extra bandwidth, which may in turn reduce the effective service rate. Thus, the FEC code rate has a subtle effect on the CLR. In general, adaptive coding yields the optimal throughput for a channel with variable error statistics [22].

In this study, we address the problem of finding an optimal bandwidth and FEC code rate for a guaranteed CLR. We refer to this bandwidth as the *wireless effective bandwidth*, which is similar in concept to the effective bandwidth in wireline ATM networks. To compute the wireless effective bandwidth, we first evaluate the cell loss performance at the transmitter, taking into account the channel behavior and the underlying error control schemes (ARQ and/or FEC). For this purpose, we model each traffic source by an on-off fluid process, and we use a fluid version of Gilbert-Elliott model to capture the behavior of the wireless channel. Using fluid-flow analysis, we compute the CLR due to buffer overflow for a single and multiplexed streams. In the single-stream case, we provide a closed-form approximation of the wireless effective bandwidth. Our results are used to study the impact of FEC on the effective bandwidth for a guaranteed CLR. Extensive simulations are conducted to verify the goodness of our analytical results.

The rest of the paper is organized as follows. In Section 2 we describe the general framework of our study. The cell loss performance for a single stream is studied in Section 3. The corresponding wireless effective bandwidth is analyzed in Section 4. The CLR for multiplexed streams is studied in Section 5. Numerical results and simulations are reported in Section 6, followed by concluding remarks in Section 7.

2 Wireless ATM Link Model

In order to analyze the cell-level performance of a wireless ATM link, we consider the framework shown in Figure 2. In this framework, traffic streams from one or more ATM connections are fed into a finite-size FIFO buffer. The buffer is drained at a constant rate c (in cells/second), which corresponds to the capacity of an error-free wireless channel. A combination of ARQ and FEC is used to improve the transport performance of the wireless link. Several hybrid ARQ/FEC mechanisms have been proposed in the wireless literature [6, 14], which cannot all be captured in one model. In our study, we consider a particular hybrid ARQ/FEC approach in which the cyclic redundancy check (CRC) code is first applied to a cell, followed by FEC (i.e., the input to the FEC coder consists of the original cell plus its CRC code). This ordering of the CRC and FEC coders has been used in several previous studies (see [23], for example). Figure 3 depicts the structure of a cell with CRC and FEC codes. We assume that the CRC code can alone detect all bit errors in a cell. In contrast, only a subset of the errors can be corrected by FEC. Note that the purpose of FEC here is to reduce the number of retransmissions, and consequently the per-stream allocated bandwidth (as demonstrated in this paper). Another application of ARQ/FEC, which is not considered here, involves a CRC code with a partial error detection capability (in this case, FEC improves the overall error *detection* rate). We focus on the tuning of the FEC coder, treating the original cell and its CRC code as payload from the standpoint of the FEC coder. For simplicity, we ignore the overhead of the medium access control (MAC) layer.

At the receiver side, an arriving cell is passed through a FEC decoder, followed by a CRC decoder. If one or more bit errors are detected by the CRC decoder, then a negative acknowledgement (NAK) is sent back to the sender. The sender must then retransmit the errored cell. In this

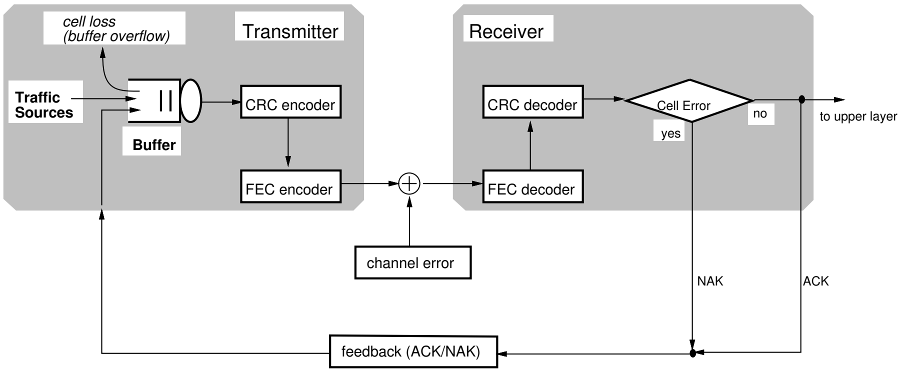

Figure 2: Framework for analyzing the performance over a wireless ATM link.

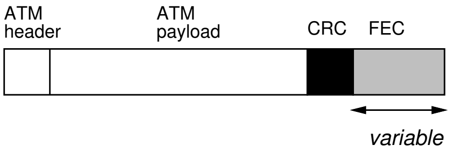

Figure 3: Cell format in wireless ATM with hybrid ARQ/FEC error control.

study, we do not impose a limit on the number of cell retransmissions, since we are mainly interested in the cell loss performance. Imposing such a limit can be used to provide delay guarantees for real-time traffic. This will be the topic of a future paper.

The above model has two control parameters: the service rate (or assigned bandwidth) and the FEC code rate. These parameters can be adjusted during connection setup to satisfy certain QoS requirements. From the network point of view, the selection of these parameters is very crucial and requires thorough understanding of their impact on the cell-level performance. The main theme of this study is to investigate the cell loss behavior of a wireless ATM link as a function of the assigned bandwidth and error control schemes.

3 Cell Loss Performance for a Single Stream

In this section, we analyze the cell loss performance for a single traffic stream transported over a wireless ATM link. The traffic source is characterized by an on-off fluid model, with peak rate r and with exponentially distributed on and off periods with means $1/\alpha$ and $1/\beta$, respectively. The wireless channel is modeled using a fluid version of Gilbert-Elliott model. This model is often used to investigate the performance of wireless links [10, 13]. As explained in Figure 4, Gilbert-Elliott model is Markovian with two alternating states: *Good* and *Bad*. The bit error rates (BER) during the Good and Bad states are given by P_{eg} and P_{eb}, respectively, where $P_{eg} \ll P_{eb}$. The durations of the Good and Bad states are exponentially distributed with means $1/\delta$ and $1/\gamma$, respectively.

The FEC capability in the underlying hybrid ARQ/FEC mechanism is characterized by three

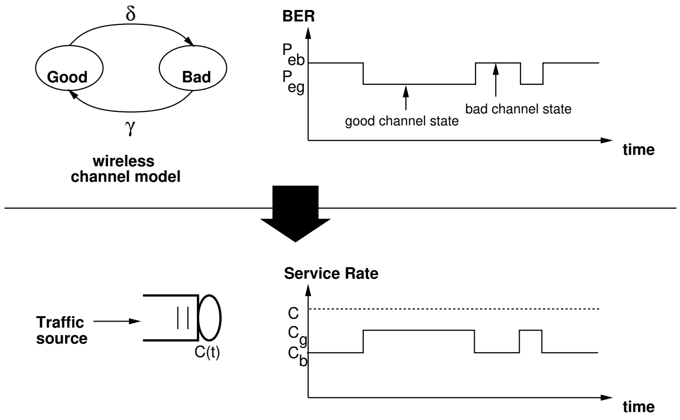

Figure 4: Wireless channel model and corresponding service rate model.

parameters: the number of bits in a code block (n), the number of payload bits (k), and the maximum number of correctable bits in a code block (τ). Note that n consists of the k payload bits and the extra parity bits. The FEC code rate $e(\tau)$ is defined as

$$e(\tau) = \frac{k}{n(\tau)}.$$

Assuming that a FEC code can correct up to τ bits and that bit errors during a given channel state are independent, the probability that a cell contains a non-correctable error is given by:

$$P_c(p_b, \tau) = \sum_{j=\tau+1}^{n(\tau)} \binom{n(\tau)}{j} p_b^j (1 - p_b)^{n(\tau)-j} \tag{1}$$

where p_b is the bit error probability; $p_b \in \{P_{eg}, P_{eb}\}$. To account for the FEC overhead, we obtain the actual service rate c_e observed at the output of the buffer:

$$c_e = c \cdot e(\tau) \tag{2}$$

where c is the bandwidth assigned to the ATM connection.

Incorporating the exact behavior of ARQ and FEC in the underlying queuing model leads to intractable results. In particular, the exact ARQ behavior gives rise to a complicated service process (even in the case of a simple stop-and-wait ARQ, the service process is a Markov-modulated Bernoulli process). Therefore, approximations are needed. To obtain analytically tractable results, we assume that the cell departure process follows a fluid process with a service rate that is modulated by the channel state (see Fig. 4). This approximation implies that there are two deterministic service rates: c_g during Good states and c_b during Bad states. We assume that the feedback delay for sending an acknowledgment from the receiver to the sender is smaller than the transmission time of a cell. We further assume that the sender attempts to retransmit a cell

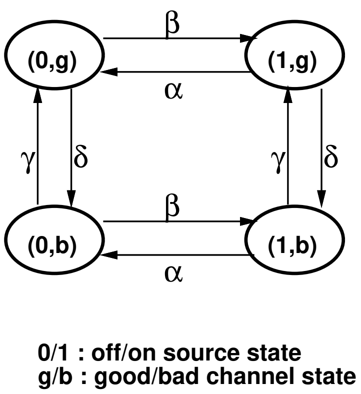

Figure 5: State transition diagram.

until this cell is successfully received (i.e., number of bit errors is less than τ). In a realistic stop-and-wait ARQ scenario, the total time needed to successfully transmit a cell has a conditional geometric distribution (conditioned on the channel state). In this case, c_g and c_b correspond to the mean values of geometric distributions with parameters $1 - P_{c,g}$ and $1 - P_{c,b}$, respectively, where $P_{c,g}$ and $P_{c,b}$ are the cell error probabilities in Good and Bad states, respectively, given by (1). Formally,

$$c_g = c \cdot e(\tau) \cdot (1 - P_{c,g}) = c \cdot e(\tau) \cdot (1 - P_c(P_{eg}, \tau)) \tag{3}$$

$$c_b = c \cdot e(\tau) \cdot (1 - P_{c,b}) = c \cdot e(\tau) \cdot (1 - P_c(P_{eb}, \tau)). \tag{4}$$

It can be seen that the problem of determining the wireless effective bandwidth reduces to obtaining a service rate c that satisfies a required CLR. The system is Markovian with a state transition diagram that is shown in Figure 5. Let S denote the state space. Thus,

$$S = \{(0, g), (1, g), (0, b), (1, b)\}$$

where 0 and 1 denote the on and off states of a traffic source, respectively, and g and b denote Good and Bad channel states, respectively.

Following a standard fluid approach (see [4], for example), the evolution of the buffer content can be described by the following differential equation:

$$\frac{d\mathbf{\Pi}(x)}{dx}\boldsymbol{D} = \mathbf{\Pi}(x)\boldsymbol{M} \tag{5}$$

where $\boldsymbol{D} \stackrel{\triangle}{=} \mathrm{diag}[-c_g, -c_b, r - c_g, r - c_b]$, $\mathbf{\Pi}(x) \stackrel{\triangle}{=} [\ \Pi_{0,g}(x) \quad \Pi_{0,b}(x) \quad \Pi_{1,g}(x) \quad \Pi_{1,b}(x)\ ], \Pi_s(x) \stackrel{\triangle}{=}$ $\Pr\{\text{buffer content} \leq x, \text{and the system } s \in S\}$, and $\boldsymbol{M}$ is the generator matrix of the underlying

Markov chain:

$$\boldsymbol{M}=\begin{bmatrix} -(\beta+\delta) & \delta & \beta & 0 \\ \gamma & -(\beta+\gamma) & 0 & \beta \\ \alpha & 0 & -(\alpha+\delta) & \delta \\ 0 & \alpha & \gamma & -(\alpha+\gamma) \end{bmatrix}.$$

Throughout the paper, matrices and vectors are boldfaced.

The solution of (5) corresponds to the solution of the eigenvalue/eigenvector problem:

$$z\boldsymbol{\phi}\boldsymbol{D}=\boldsymbol{\phi}\boldsymbol{M} \tag{6}$$

which is generally given by

$$\boldsymbol{\Pi}(x)=\sum_{z_i\leq 0} a_i \exp(z_i x)\phi_i \tag{7}$$

where a_i's are constant coefficients and the pairs $(z_i,\boldsymbol{\phi}_i), i=1,2,\cdots$, are the eigenvalues and the right eigenvectors of the matrix $\boldsymbol{M}\boldsymbol{D}^{-1}$ [4, 18]. Let $\boldsymbol{w}$ denote the stationary probability vector of the Markov chain; $\boldsymbol{w}$ satisfies $\boldsymbol{w}\boldsymbol{M}=0$ and $\boldsymbol{w}\mathbf{1}=1$, where $\mathbf{1}$ is a column vector of ones. Then $\boldsymbol{w}$ is given by:

$$\boldsymbol{w}=\frac{1}{(\alpha+\beta)(\delta+\gamma)}\begin{bmatrix} \alpha\gamma & \alpha\delta & \beta\gamma & \beta\delta \end{bmatrix}. \tag{8}$$

The mean drift is given by:

$$\boldsymbol{w}\boldsymbol{D}\mathbf{1}=\frac{\beta}{\alpha+\beta}r-\frac{c_g\gamma+c_b\delta}{\delta+\gamma}. \tag{9}$$

For a stable system, $\boldsymbol{w}\boldsymbol{D}\mathbf{1}<0$. In this paper, we consider a stable system with an infinite buffer.

In order to solve (6), we follow the approach used in [18]. The four-state Markov process is decomposed into two processes; one describes the on-off source and the other describes the state of the channel. These two processes are parameterized by the two generator matrices $\boldsymbol{M}_1$ and $\boldsymbol{M}_2$, where

$$\boldsymbol{M}_1=\begin{bmatrix} -\beta & \beta \\ \alpha & -\alpha \end{bmatrix} \text{ and } \boldsymbol{M}_2=\begin{bmatrix} -\delta & \delta \\ \gamma & -\gamma \end{bmatrix} \tag{10}$$

with

$$\boldsymbol{M}=\boldsymbol{M}_1\otimes\boldsymbol{I}+\boldsymbol{I}\otimes\boldsymbol{M}_2 \tag{11}$$

and $\boldsymbol{A} \otimes \boldsymbol{B}$ is the Kronecker product of two matrices $\boldsymbol{A}$ and $\boldsymbol{B}$. For the drift matrix $\boldsymbol{D}$, we have

$$\boldsymbol{D} = r\boldsymbol{E}_r \otimes \boldsymbol{I} - \boldsymbol{I} \otimes \boldsymbol{E}_c \tag{12}$$

where $\boldsymbol{E}_r$ and $\boldsymbol{E}_c$ are given by

$$\boldsymbol{E}_r = \begin{bmatrix} 0 & 0 \\ 0 & 1 \end{bmatrix} \text{ and } \boldsymbol{E}_c = \begin{bmatrix} c_g & 0 \\ 0 & c_b \end{bmatrix}. \tag{13}$$

Consider the following decomposition for the eigenvector of $\boldsymbol{M}\boldsymbol{D}^{-1}$:

$$\boldsymbol{\phi} = \boldsymbol{\phi}_1 \otimes \boldsymbol{\phi}_2 \tag{14}$$

where $\boldsymbol{\phi}_1$ and $\boldsymbol{\phi}_2$ are two dimensional vectors.

On substituting the expressions for $\boldsymbol{D}$, $\boldsymbol{M}$, and $\boldsymbol{\phi}$ from (12), (11), (14) into (6), we end up with

$$\boldsymbol{\phi}_1 \otimes (\boldsymbol{\phi}_2 \boldsymbol{M}_2 + z\boldsymbol{\phi}_2 \boldsymbol{E}_c) = (zr\boldsymbol{\phi}_1 \boldsymbol{E}_r - \boldsymbol{\phi}_1 \boldsymbol{M}_1) \otimes \boldsymbol{\phi}_2. \tag{15}$$

Hence, for (6) and (14) to be valid, it is sufficient that there exists some real number v such that both sides of the above equation equal $zv\boldsymbol{\phi}_1 \otimes \boldsymbol{\phi}_2$:

$$z\boldsymbol{\phi}_1[r\boldsymbol{E}_r - v\boldsymbol{I}] \quad = \quad \boldsymbol{\phi}_1 \boldsymbol{M}_1 \tag{16}$$

$$z\boldsymbol{\phi}_2[v\boldsymbol{I} - \boldsymbol{E}_c] \quad = \quad \boldsymbol{\phi}_2 \boldsymbol{M}_2 \tag{17}$$

which implies that

$$\begin{aligned} \det[z\boldsymbol{I} - \boldsymbol{M}_1[r\boldsymbol{E}_r - v\boldsymbol{I}]^{-1}] &= 0 \\ \det[z\boldsymbol{I} - \boldsymbol{M}_2[v\boldsymbol{I} - \boldsymbol{E}_c]^{-1}] &= 0 \end{aligned} \tag{18}$$

where $\det[\boldsymbol{A}]$ is the determinant of $\boldsymbol{A}$. The first equation in (18) reduces to the quadratic polynomial

$$(zv)^2 - (zr + \alpha + \beta)zv + \beta zr = 0. \tag{19}$$

Thus,

$$zv = \frac{zr + \alpha + \beta}{2} \pm \frac{\sqrt{Q_1(z)}}{2} \tag{20}$$

where

$$Q_1(z) = (zr + \alpha - \beta)^2 + 4\alpha\beta. \tag{21}$$

For the second equation in (18), we have

$$(zv)^2 - (z(c_g + c_b) - \delta - \gamma)zv + z(zc_gc_b - \gamma c_g - \delta c_b) = 0. \tag{22}$$

Thus,

$$zv = \frac{z(c_g + c_b) - \delta - \gamma}{2} \pm \frac{\sqrt{Q_2(z)}}{2} \tag{23}$$

where

$$Q_2(z) = (z(c_g - c_b) - (\delta - \gamma))^2 + 4\delta\gamma. \tag{24}$$

Equating (20) and (23) leads to the following four equations that provide four distinct eigenvalues:

$$\begin{aligned}
z(r - c_g - c_b) + \alpha + \beta + \delta + \gamma + \sqrt{Q_1(z)} + \sqrt{Q_2(z)} &= 0 \\
z(r - c_g - c_b) + \alpha + \beta + \delta + \gamma + \sqrt{Q_1(z)} - \sqrt{Q_2(z)} &= 0 \\
z(r - c_g - c_b) + \alpha + \beta + \delta + \gamma - \sqrt{Q_1(z)} + \sqrt{Q_2(z)} &= 0 \\
z(r - c_g - c_b) + \alpha + \beta + \delta + \gamma - \sqrt{Q_1(z)} - \sqrt{Q_2(z)} &= 0.
\end{aligned}$$

From the above set of equations, we can establish the following equation to eliminate the square roots:

$$((z(r - c_g - c_b) + \alpha + \beta + \delta + \gamma)^2 - Q_1(z) - Q_2(z))^2 - 4Q_1(z)Q_2(z) = 0. \tag{25}$$

Rearranging (25), we obtain a polynomial equation of order three, whose solutions correspond to the three nonzero eigenvalues (see Appendix A for details).

After obtaining the eigenvalues, the corresponding values for v can be obtained using (20) and (23). Once z and v are determined, the corresponding eigenvectors can be obtained from (16) and (17):

$$\boldsymbol{\phi}_1 = [\ \alpha \quad -zv + \beta\ ] \tag{26}$$

$$\boldsymbol{\phi}_2 = [\ \gamma \quad zv - zc_g + \delta\ ]. \tag{27}$$

Thus,

$$\boldsymbol{\phi} = \boldsymbol{\phi}_1 \otimes \boldsymbol{\phi}_2 = [\ \alpha\gamma \quad \alpha(zv - zc_g + \delta) \quad (-zv + \beta)\gamma \quad (-zv + \beta)(zv - zc_g + \delta)\ ]. \tag{28}$$

Finally, the stationary buffer content distribution $\mathbf{\Pi}(x)$ is given by

$$\mathbf{\Pi}(x) = a_d \boldsymbol{w} + \sum_{z_i < 0} a_i \exp(z_i x) \boldsymbol{\phi}_i \tag{29}$$

where a_d is the coefficient associated with the zero eigenvalue. For a stable system, the coefficients a_i associated with positive eigenvalues are set to zero.

For an infinite buffer system, we have the following boundary conditions [18]:

$$\begin{aligned} \Pi_s(0) &= 0, \quad \text{for } z_i < 0, \text{with } r > c_g, r > c_b \\ a_d &= 1, \quad (\text{since } \mathbf{\Pi}(\infty) = \boldsymbol{w}). \end{aligned}$$

If $r > c_g$, we have two negative eigenvalues, z_1 and z_2. In this case, the coefficients are given by

$$\begin{bmatrix} a_1 \\ a_2 \end{bmatrix} = - \begin{bmatrix} \phi_{1g}(z_1) & \phi_{1g}(z_2) \\ \phi_{1b}(z_1) & \phi_{1b}(z_2) \end{bmatrix}^{-1} \begin{bmatrix} w_{1g} \\ w_{1b} \end{bmatrix} \tag{30}$$

where $\phi_s(z)$ is the eigenvector element of state s by (28).

If $r < c_g$, there is only one negative eigenvalue z_1. The coefficient a_1 is simply given by:

$$a_1 = -w_{1b}/\phi_{1b}(z_1). \tag{31}$$

After obtaining the eigenvalues, the eigenvectors, and the coefficients, we can construct the stationary buffer content distribution $\mathbf{\Pi}(x)$. Consequently, the CLR due to buffer overflow $G(x)$ is given by:

$$G(x) \quad = \quad 1 - \mathbf{1}\mathbf{\Pi}(x). \tag{32}$$

In Section 6, we provide some numerical results related to the CLR. In addition, we compare the above analytic result with simulation results to test the accuracy of our analysis.

4 Wireless Effective Bandwidth

The expression for the CLR that was obtained in the previous section can, in principle, be used to compute the effective bandwidth. However, this requires expressing the service rate c as a function of other variables (CLR, buffer size, channel BERs, the number of correctable bits, etc.). In general, it is not possible to obtain an *exact* closed-form expression for the effective bandwidth, which would be useful in real-time traffic control [1]. Even for a single source (i.e., no multiplexing), the closed-form solution is not available without approximation [7, 12].

In this section, we derive an approximate expression for the effective bandwidth following the approach used in [8]. In [8] the authors consider the service rate c to be a variable parameter and the eigenvalues to be functions of c, i.e., $z = f(c)$. Since the problem is to obtain c for a given z, c can be expressed as the inverse function, i.e., $c = f^{-1}(z) \triangleq g(z)$. The key point in the analysis is that this inversion problem reduces to another eigenvalue problem (see [8] for details).

Consider (6). In this case, the drift matrix $\boldsymbol{D}$ can be written as

$$\boldsymbol{D} = r\boldsymbol{B}_r - ce(\tau)\boldsymbol{B}_c$$

where

$$\boldsymbol{B}_r = \begin{bmatrix} 0 & 0 & 0 & 0 \\ 0 & 0 & 0 & 0 \\ 0 & 0 & 1 & 0 \\ 0 & 0 & 0 & 1 \end{bmatrix}, \boldsymbol{B}_c = \begin{bmatrix} \eta_g & 0 & 0 & 0 \\ 0 & \eta_b & 0 & 0 \\ 0 & 0 & \eta_g & 0 \\ 0 & 0 & 0 & \eta_b \end{bmatrix} \tag{33}$$

$\eta_g = 1 - P_c(P_{eg}, \tau)$, and $\eta_b = 1 - P_c(P_{eb}, \tau)$. Substituting $\boldsymbol{D}$ into (6), we obtain the following relation:

$$z\boldsymbol{\phi}(r\boldsymbol{B}_r - ce(\tau)\boldsymbol{B}_c) \;=\; \boldsymbol{\phi}\boldsymbol{M}. \tag{34}$$

Let $c \triangleq g(z)$. Then,

$$zr\boldsymbol{\phi}\boldsymbol{B}_r - zg(z)e(\tau)\boldsymbol{\phi}\boldsymbol{B}_c \;=\; \boldsymbol{\phi}\boldsymbol{M}. \tag{35}$$

Rearranging the previous equation, we obtain

$$g(z)e(\tau)\boldsymbol{\phi} \;=\; \boldsymbol{\phi}\left(-\frac{1}{z}\boldsymbol{M} + r\boldsymbol{B}_r\right)\boldsymbol{B}_c^{-1}. \tag{36}$$

Note that the problem of obtaining $g(z)$ translates into another eigenvalue problem. According to [8], the effective bandwidth is approximated by the maximal eigenvalue $g(z)$ satisfying (36).

From (36) and after some tedious algebraic manipulations, we obtain the following four eigen-

[1]In this paper, we use the term 'effective bandwidth' in a general sense to refer to the minimum service capacity that is needed to achieve a given CLR. We use the term 'effective bandwidth approximation' to refer to the more specific definition of Elwalid et al. [8].

values:

$$g(z)e(\tau) = \begin{cases} \frac{C_1-(\eta_g+\eta_b)C_2 \pm \sqrt{2(C_3-C_2C_4)}}{4\eta_g\eta_b} \\ \frac{C_1+(\eta_g+\eta_b)C_2 \pm \sqrt{2(C_3+C_2C_4)}}{4\eta_g\eta_b} \end{cases}$$

where

$$\begin{aligned} C_1 &= (\eta_g+\eta_b)r - ((\alpha+\beta+2\gamma)\eta_g + (\alpha+\beta+2\delta)\eta_b)\xi \\ C_2 &= \sqrt{(r-(\alpha-\beta)\xi)^2 + 4\alpha\beta\xi^2} \\ C_3 &= \eta_b^2((r-(\alpha+\delta)\xi)^2 + ((\beta+\delta)^2+2\alpha\beta)\xi^2) \\ &\quad -2\eta_g\eta_b(r^2-(2\alpha+\delta+\gamma)r\xi + ((\alpha+\beta)(\alpha+\beta+\delta+\gamma)-2\delta\gamma)\xi^2) \\ &\quad +\eta_g^2((r-(\alpha+\gamma)\xi)^2 + ((\beta+\gamma)^2+2\alpha\beta)\xi^2) \\ C_4 &= (\eta_g-\eta_b)(\eta_g(r-(\alpha+\beta+2\gamma)\xi) - \eta_b(r-(\alpha+\beta+2\delta)\xi)) \\ \xi &= -B/\log p,\ B \text{ is buffer size and } p \text{ is CLR.} \end{aligned}$$

Thus, the maximal eigenvalue, corresponding to the wireless effective bandwidth approximation, is given by:

$$g(z) = \frac{C_1+(\eta_g+\eta_b)C_2+\sqrt{2(C_3+C_2C_4)}}{4\eta_g\eta_b e(\tau)}. \tag{37}$$

Note that this is an asymptotic result, i.e., the buffer size is very large and the CLR is very small.

5 Cell Loss Performance for Multiplexed Streams

So far, we have considered the transport of a single on-off source over a wireless ATM link. As indicated in Figure 1, it is also possible to multiplex several connections onto the same wireless link. In this section, we extend our previous cell loss analysis to the case of multiplexed streams.

The wireless ATM link is modeled as an ATM multiplexer with randomly varying service rate. This model is similar to the producer-consumer model investigated in [18]. In [18] the traffic generation (production) and the cell delivery (consumption) processes are coupled by a buffer, which enables their decomposition and consequently facilitates the analysis. When a single connection is considered, the traffic generation and delivery processes are specified by Equations (16) and (17), respectively. For K multiplexed Markovian fluid sources, the traffic generation part is governed by the following equation [18]:

$$z\boldsymbol{\phi}_s[\boldsymbol{\Lambda}_s - v\boldsymbol{I}] = \boldsymbol{\phi}_s\boldsymbol{M}_s \tag{38}$$

where $\boldsymbol{M}_s$ and $\boldsymbol{\Lambda}_s$ are the infinitesimal generator and rate matrices for the aggregate traffic, respectively. These matrices can be written as

$$\begin{aligned}\boldsymbol{M}_s &= \boldsymbol{M}_1 \oplus \boldsymbol{M}_2 \oplus \cdots \oplus \boldsymbol{M}_K \\ \boldsymbol{\Lambda}_s &= \boldsymbol{\Lambda}_1 \oplus \boldsymbol{\Lambda}_2 \oplus \cdots \oplus \boldsymbol{\Lambda}_K\end{aligned}$$

where $\boldsymbol{M}_i$ and $\boldsymbol{\Lambda}_i$ are the infinitesimal generator and rate matrices of the ith source, $i = 1, 2, \cdots, K$. In (38), z and $\boldsymbol{\phi}_s$ are the eigenvalue and eigenvector of the matrix $\boldsymbol{M}_s[\boldsymbol{\Lambda}_s - v\boldsymbol{I}]^{-1}$, respectively. The operator $\oplus$ denotes the Kronecker sum.

As for the cell delivery process, it is governed by [18]:

$$z\boldsymbol{\phi}_r[v\boldsymbol{I} - \boldsymbol{E}_c] = \boldsymbol{\phi}_r \boldsymbol{M}_r \tag{39}$$

where $\boldsymbol{M}_r$ is the generator matrix for the service process (the consumption part), and z and $\boldsymbol{\phi}_r$ are the corresponding eigenvalue and eigenvector, respectively. For the two-state Gilbert-Elliott channel model, $\boldsymbol{M}_r$ and $\boldsymbol{E}_c$ correspond to $\boldsymbol{M}_2$ in (10) and $\boldsymbol{E}_c$ in (13), respectively.

Exact analysis of the producer-consumer system described by (38) and (39) was provided in [18] for on-off sources. The buffer consumption rates in [18] were taken as integer multiples of some unit rate. In Appendix B, we provide the exact solution for the CLR based on Mitra's results, with adaptation to our wireless ATM model. Note that in our model, there are two consumption rates (c_b and c_g). But c_g is not necessarily an integer multiple of c_b.

While an exact solution for the CLR is feasible, the computational complexity associated with this solution is rather high. A much simpler approximate solution can be obtained, which is sufficiently accurate. In [9], Elwalid et al. proposed an approximation for the CLR at an ATM multiplexer for general Markovian sources using a combined Chernoff-dominant eigenvalue (CDE) approach. In this approximation, the CLR at the multiplexer with buffer size x is approximated by

$$G(x) \approx Le^{zx} \tag{40}$$

where z is the dominant eigenvalue and L is the corresponding coefficient. A procedure was presented for computing z and L for an ATM multiplexer with a constant service rate c. A similar procedure will be used in this paper to approximate the CLR at a wireless ATM link. Note that the service rate in our model fluctuates randomly depending on the channel state.

5.1 Calculation of the Dominant Eigenvalue

According to the results in [8], the dominant eigenvalue of (38) is the unique solution of the equation:

$$\sum_{i=1}^{K} g_i(z) = v \tag{41}$$

where $g_i(z) =$ MRE$[\mathbf{\Lambda}_i - \boldsymbol{M}_i/z]$ and MRE$[\boldsymbol{A}]$ denotes the maximal real eigenvalue of the matrix $\boldsymbol{A}$. Note that v is a variable coupling (38) and (39), which differs from [8] in that the constant service rate in [8] is replaced by the variable v. Let us consider the cell delivery part corresponding to (39). From (23), v is given by

$$v = \frac{z(c_g + c_b) - \delta - \gamma \pm \sqrt{Q_2(z)}}{2z}. \tag{42}$$

We can obtain the dominant eigenvalue by equating the left-hand side of (41) and the right-hand side of (42). Since the dominant eigenvalue is the unique solution of (41) and z is a decreasing function in v, the smaller value of v in (42), i.e., the term containing $+\sqrt{Q_2(z)}$, must be equated with (41) to obtain the dominant eigenvalue:

$$\sum_{i=1}^{K} g_i(z) = \frac{z(c_g + c_b) - \delta - \gamma + \sqrt{Q_2(z)}}{2z}. \tag{43}$$

Thus, the following proposition can be established.

Proposition 5.1 *The dominant eigenvalue in the wireless ATM multiplexer model represented by (38) and (39) is the value of z satisfying the following equation:*

$$\sum_{i=1}^{K} g_i(z) = \frac{z(c_g + c_b) - \delta - \gamma + \sqrt{Q_2(z)}}{2z}. \tag{44}$$

For a single on-off source, $g(z)$ is given by:

$$g(z) = \frac{(rz + \alpha + \beta) - \sqrt{(rz + \alpha - \beta)^2 + 4\alpha\beta}}{2z}$$

which is the same as (20).

5.2 Approximation of the Coefficient L Using Chernoff-Bound Approach

Prior studies have shown that the coefficient L in (40) plays a critical role in obtaining an accurate estimate of the CLR [7, 9]. In this section, we provide an approximation of L using a Chernoff-bound approach, in line of Elwalid et al.'s work [9] on analyzing the CLR at a multiplexer with a constant drain rate.

Following the discussion in [9] and the references therein, one can approximate the constant L by $G(0)$, implying that L is *approximately* the cell loss probability in a bufferless multiplexer:

$$G(0) \approx L. \tag{45}$$

In a bufferless multiplexer, cell losses occur when the input rate exceeds the service rate. Let χ_i denote the cell rate from source i at steady-state. The total traffic generation rate from K sources is denoted by χ where $\chi = \sum_{i=1}^{K} \chi_i$. For an ATM multiplexer with a fixed service rate R, L is estimated by

$$L \approx P[\chi \geq R].$$

Using Chernoff bound, Elwalid et al. [9] showed that as $R \to \infty$ with $K/R = o(1)$, $P[\chi \geq R]$ can be obtained as follows:

$$P[\chi \geq R] = \frac{\exp(-F(s^*))}{s^*\sigma(s^*)\sqrt{2\pi}}[1 + o(1)] \tag{46}$$

where

$$\begin{aligned} F(s) &\triangleq sR - \sum_{i=1}^{K} \log N_i(s) &(47)\\ N_i(s) &\triangleq E[\exp(s\chi_i)] &(48)\\ \sigma^2(s) &= \frac{\partial^2 \log E[\exp(s\chi)]}{\partial s^2} \\ &= \sum_{i=1}^{K} \left[\frac{N_i''(s)}{N_i(s)} - \left(\frac{N_i'(s)}{N_i(s)} \right)^2 \right] &(49) \end{aligned}$$

and $F(s^*) = \sup_{s \geq 0} F(s)$.

In our case, R is not fixed, but can take one of two values (c_g and c_b). Losses will occur when χ exceeds c_g during the Good state and c_b during the Bad state. Thus, L in (40) is given by:

$$L \approx G(0) = P[\chi \geq c_g]w_g + P[\chi \geq c_b]w_b \tag{50}$$

where w_g and w_b are the steady-state probabilities that the channel is in Good and Bad states, respectively; $w_g = \gamma/(\delta + \gamma)$, $w_b = \delta/(\delta + \gamma)$. The probabilities $P[\chi \geq c_g]$ and $P[\chi \geq c_b]$ are obtained by substituting c_g and c_b for R in (46). For K homogeneous on-off sources with a constant service rate R, we have

$$\begin{aligned} N_i(s) &= w_1 e^{sr} + w_0 \\ F(s) &= sR - K \log(w_1 e^{sr} + w_0) \end{aligned}$$

$$\sigma^2(s) = \frac{Kw_1w_0r^2e^{sr}}{(w_1e^{sr}+w_0)^2}$$

where r is the source peak rate, w_1 and w_0 are the steady-state probabilities that a source is in on and off states, respectively; $w_1 = \beta/(\alpha+\beta)$ and $w_0 = \alpha/(\alpha+\beta)$. For $R < Kr$, $F(s)$ is a concave function with s^* given by

$$s^* = \frac{1}{r}\log\frac{Rw_0}{(Kr-R)w_1}. \tag{51}$$

Replacing R in the above equation by c_g and c_b, one at a time, we obtain corresponding values s_g^* and s_b^*, which are then used in (50) to evaluate $P[\chi \geq c_g]$ and $P[\chi \geq c_b]$. In summary, for K homogeneous on-off sources that are multiplexed onto the wireless link, L is given by

$$\begin{aligned} L &= P[\chi \geq c_g]w_g + P[\chi \geq c_b]w_b \\ &= \frac{e^{-s_g^*c_g}(w_1e^{s_g^*r}+w_0)^{K+1}w_g}{s_g^*r\sqrt{2\pi Kw_1w_0e^{s_g^*r}}} + \frac{e^{-s_b^*c_b}(w_1e^{s_b^*r}+w_0)^{K+1}w_b}{s_b^*r\sqrt{2\pi Kw_1w_0e^{s_b^*r}}} \end{aligned} \tag{52}$$

6 Numerical Results and Simulations

In this section, we present numerical examples of our analytical results. We verify the adequacy of these results by contrasting them against more realistic simulations.

Similar to the analysis, the simulation results are obtained using on-off traffic sources with exponentially distributed on and off periods. However, the length of an on period in the simulations is truncated to obtain an integer number of cells. The ARQ retransmission process is simulated in a more realistic manner, whereby a cell is transmitted repeatedly until it is received with no errors. The probability of a cell error is computed from (1) for both channel states. Conditioned on the state of the channel, the number of retransmissions of a given cell in the simulation setup follows a geometric distribution. Transitions between Good and Bad states are assumed to occur only at the beginning of a cell transmission slot. A cell is retransmitted if one or more bits are in error. It is assumed that the propagation delay is small, so that the ACK/NAK message for a cell is received at the sender before the next transmission slot. Finally, we use a finite buffer size in our simulations, in contrast to the infinite-buffer assumption in the analysis.

In our experiments, we vary the buffer size and the BER during the Bad state (P_{eb}), and we fix the BER during the Good state at $P_{eg} = 10^{-6}$. We set the mean of the off period to ten times that of the on period. In addition, we take the parameters related to the wireless channel from [13]. We adopt Bose-Chaudhuri-Hocquenghem (BCH) code [16] for FEC . Since we treat the CRC code as part of the payload, the FEC code is applied to 424-bit data units (i.e., $k = 424$ bits). Table 1 shows the size, the code rate, and the number of correctable bits of the BCH code used in our examples. All simulation results are reported with 95% confidence intervals. Table 2 summarizes the values of the various parameters in the simulations and numerical examples.

(n, k)	τ	$e(\tau)$
$(442, 424)$	2	0.959
$(451, 424)$	3	0.940
$(460, 424)$	4	0.921
$(469, 424)$	5	0.904
$(478, 424)$	6	0.887

Table 1: FEC code rate versus number of correctable bits (τ) using BCH scheme.

Parameter	Symbol	Value
peak rate	r	1 Mbps (or 2604.1667 cells/sec)
buffer size	B	$100 - 1000$ cells
mean on period	$1/\alpha$	0.02304 sec
mean off period	$1/\beta$	0.2304 sec
mean Good channel period	$1/\delta$	0.1 sec
mean Bad channel period	$1/\gamma$	0.0333 sec
BER in Good channel state	P_{eg}	10^{-6}
BER in Bad channel state	P_{eb}	$10^{-2} - 10^{-5}$

Table 2: Parameter values used in the simulations and numerical results.

Figure 6 shows the CLR as a function of the buffer size using $P_{eb} = 0.01$, $\tau = 0, 4$, and $c = 500$ cells/sec. As expected, the CLR increases as the buffer size decreases and as τ decreases. It is observed that the analytic results slightly overestimate the actual CLR. The gap is negligible over the whole range of buffer sizes.

Figure 7 and 8 depict the CLR versus the buffer size using two different service rates $c = 700$ and 900 cells/sec ($P_{eb} = 10^{-2}, \tau = 0, 4$). In Figure 7, it is observed that the simulation and analytical results are quite close to each other. As c increases (Figure 8), the analytic results begin to slightly underestimate the CLR. This trend is shown clearly in Figures 9 and 10, which depict the CLR as a function of the service rate c using different buffer sizes and FEC code rates. The deviation of the analytical results is negligible, given that CLRs in ATM are contrasted in terms of the orders of magnitude by which they differ.

Figures 11, 12, and 13 depict the wireless effective bandwidth computed based on the results in Section 4. Only ARQ is used in obtaining these figures, i.e., $\tau = 0$. The case of hybrid ARQ/FEC will be discussed later. These figures depict the exact and approximate values of the wireless effective bandwidth. The exact value is obtained using all eigenvalues, while the approximate value is obtained based on the analysis in Section 4. It is observed from these figures that the wireless effective bandwidth approximation (based on one eigenvalue) is acceptable for the single stream case. However, the adequacy of this approximation does not extend to the multiplexed-streams case (not shown), as the gap between the exact and approximate solutions increases with

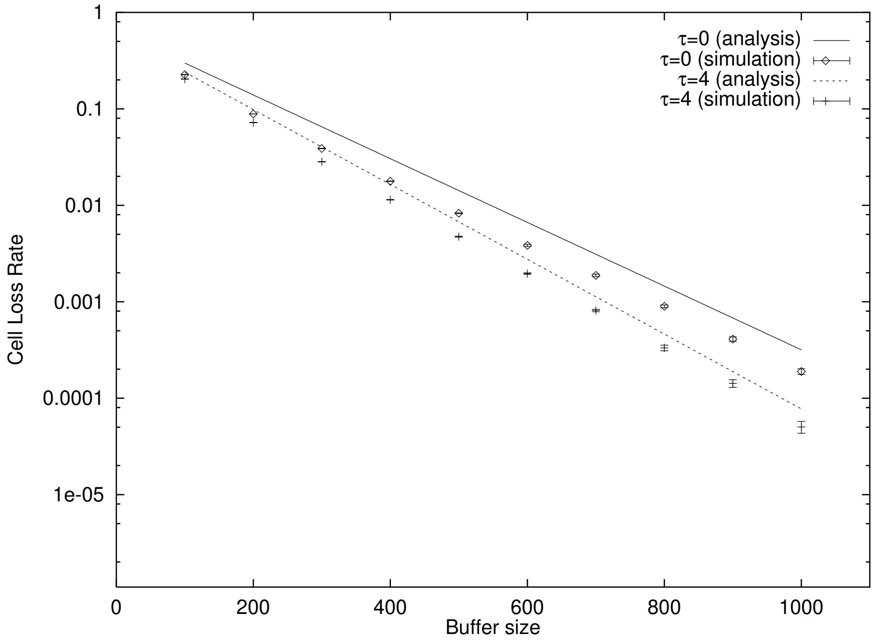

Figure 6: Cell loss rate versus buffer size for a single stream ($c = 500$, $P_{eb} = 10^{-2}$).

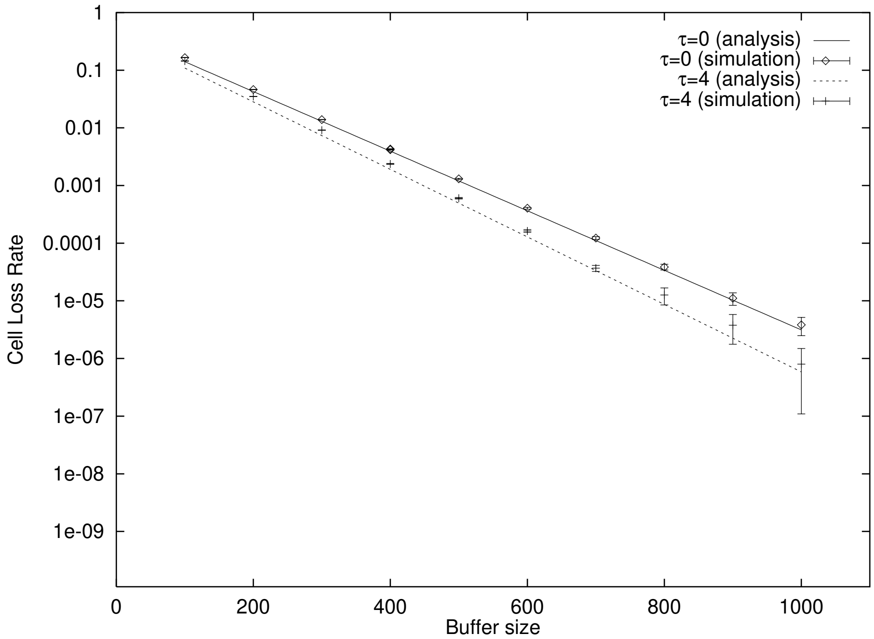

Figure 7: Cell loss rate versus buffer size for a single stream ($c = 700$ cells/sec, $P_{eb} = 10^{-2}$).

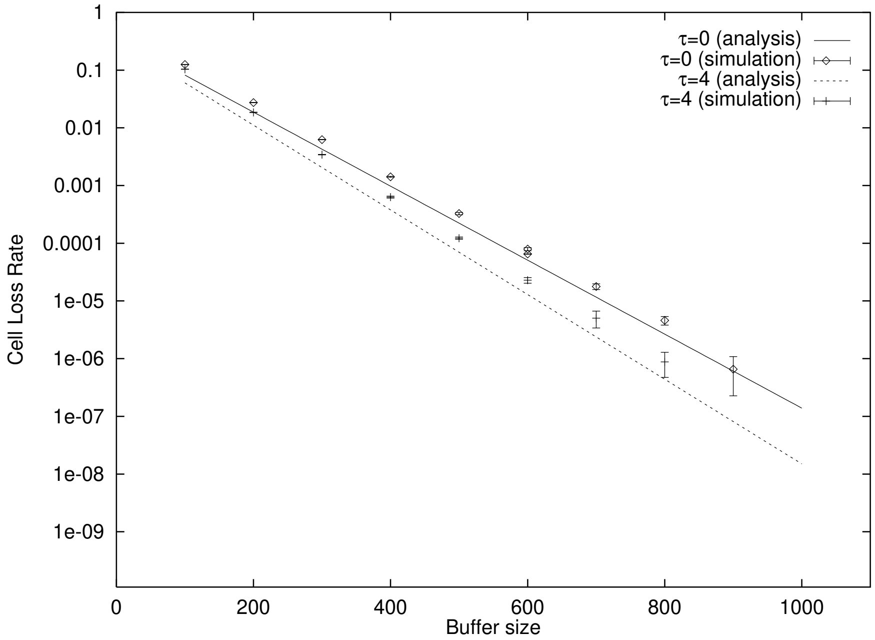

Figure 8: Cell loss rate versus buffer size for a single stream ($c = 900$ cells/sec, $P_{eb} = 10^{-2}$).

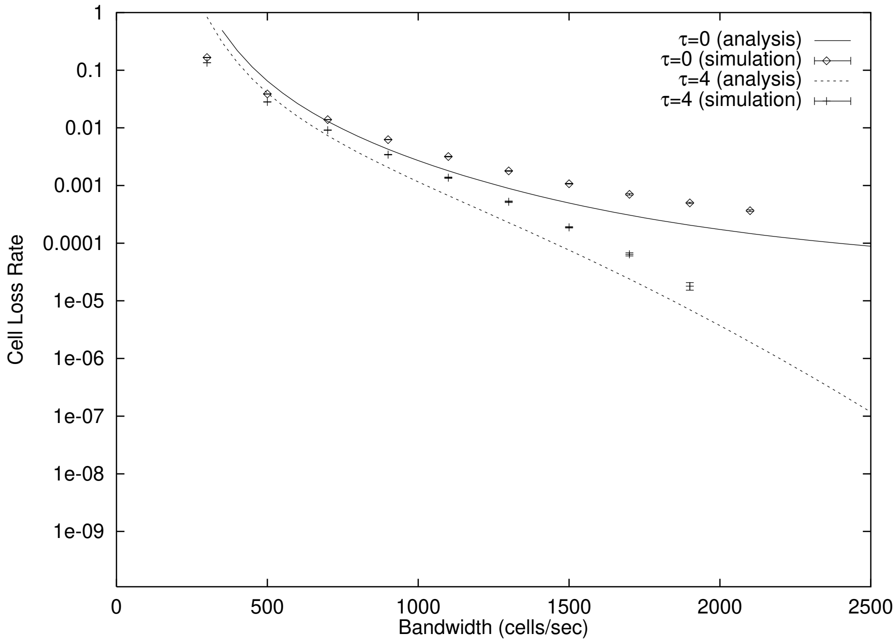

Figure 9: Cell loss rate versus service rate c for a single stream ($B = 300$, $P_{eb} = 10^{-2}$).

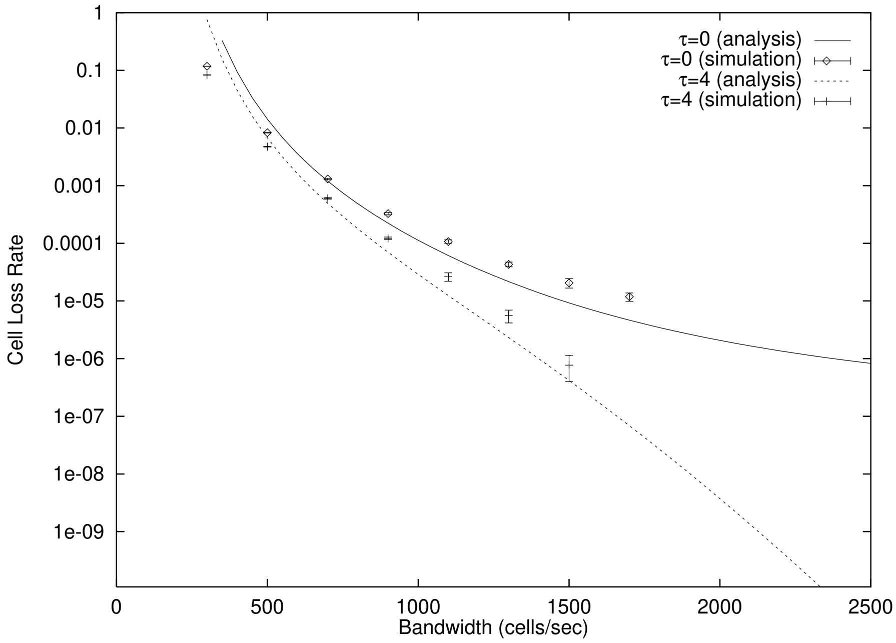

Figure 10: Cell loss rate versus service rate c for a single stream ($B = 500$, $P_{eb} = 10^{-2}$).

the number of multiplexed streams. This fact has also been observed in wireline ATM multiplexers [7]. For this reason, we restrict our effective bandwidth results to the case of a single stream.

When $P_{eb} = 10^{-4}$ and the buffer size is 300 cells, the wireless effective bandwidth ranges from 1340 to 1850 cells/sec for a CLR in the range 10^{-4} to 10^{-7}. Recall that the mean and peak rates of a traffic source are 263.74 and 2604.1667 cells/sec, respectively. As P_{eb} increases, the wireless effective bandwidth gets closer to the source peak rate. For example, when $P_{eb} = 10^{-3}$ and the buffer size is 300 cells, the wireless effective bandwidth ranges from 1501 and 2216 cells/sec for a CLR in the range 10^{-4} to 10^{-7}. For higher P_{eb} values, the wireless effective bandwidth approximation becomes less efficient, as it approaches the source peak rate.

Figure 14 depicts the wireless effective bandwidth as a function of P_{eb} for three target CLRs using $B = 800$ cells. Only ARQ is considered in obtaining this figure. It is observed that the wireless effective bandwidth increases as P_{eb} increases and as the target CLR decreases. In particular, the wireless effective bandwidth increases by a noticeable amount when P_{eb} goes from 10^{-3} to 10^{-2}. This is due to the fact that increasing P_{eb} from 10^{-3} to 10^{-2} has a relatively significant effect on the cell error probability. For example, when P_{eb} goes from 10^{-5} to 10^{-4}, the cell error probability increases from 0.004231 to 0.04151. In contrast, when P_{eb} goes from 10^{-3} to 10^{-2}, the cell error probability increases from 0.3457 to 0.9858.

Figures 15-17 show the approximate wireless effective bandwidth versus the number of correctable bits τ for different target CLRs and different BERs. The buffer size B is fixed at 800 cells. These figures indicate the existence of an "optimal" code rate at which the allocated bandwidth is minimized for a given target CLR. For instance, to provide a target CLR of 10^{-6} when

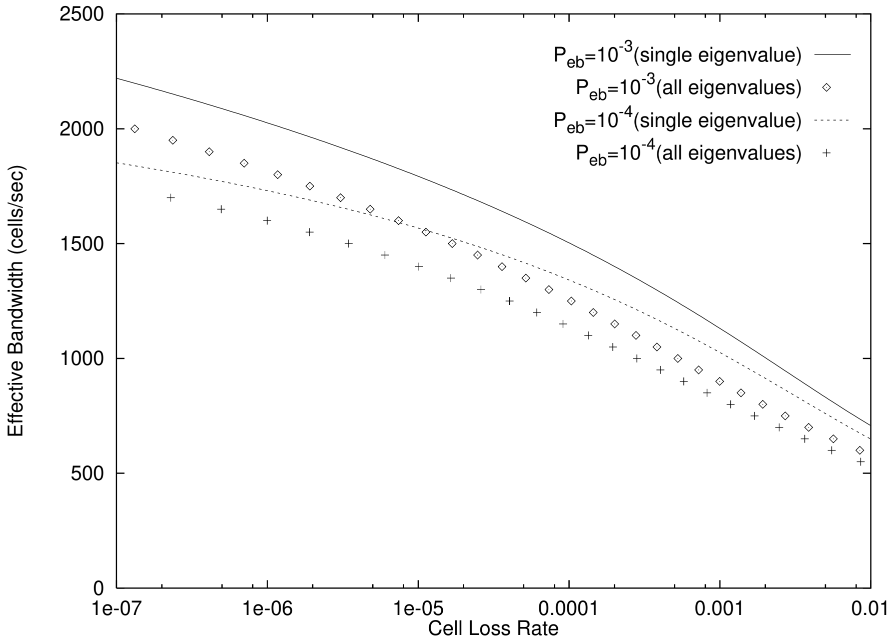

Figure 11: Effective bandwidth versus CLR for a single stream ($B = 300$, $\tau = 0$).

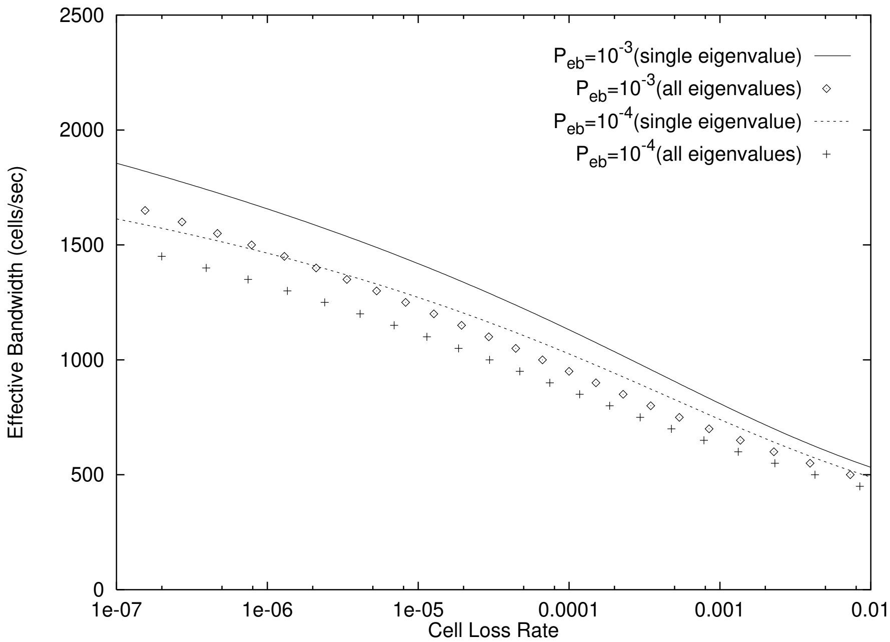

Figure 12: Effective bandwidth versus CLR for a single stream ($B = 400$, $\tau = 0$).

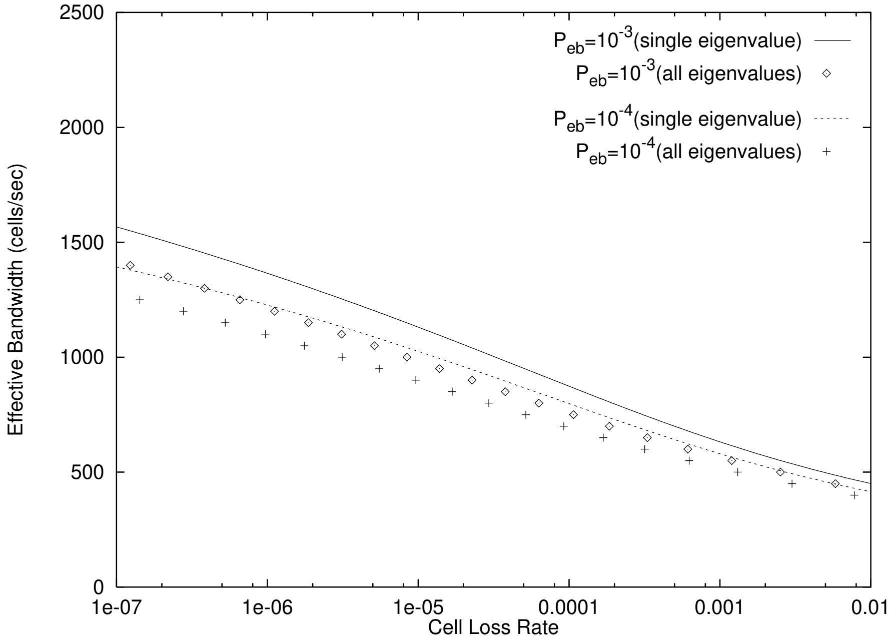

Figure 13: Effective bandwidth versus CLR for a single stream ($B = 500$, $\tau = 0$).

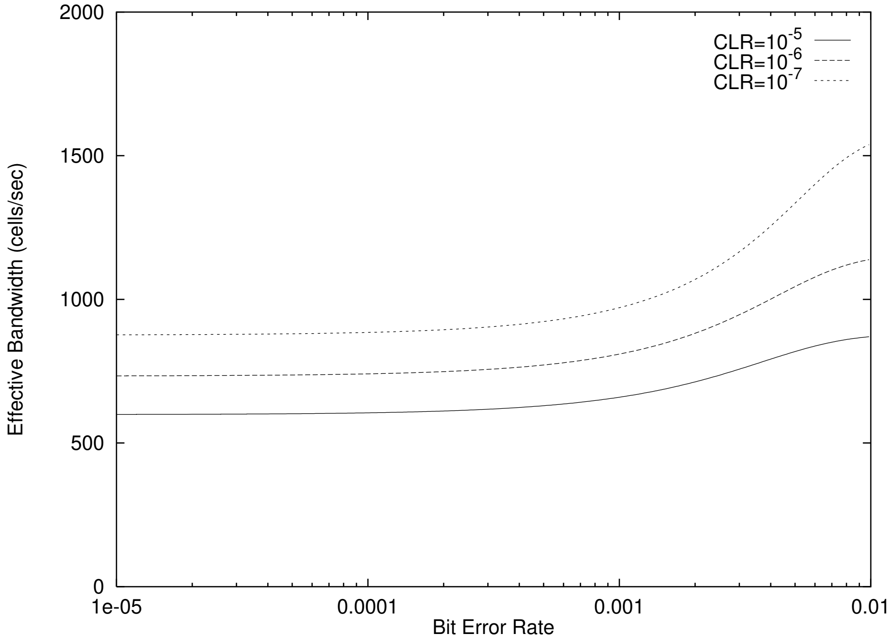

Figure 14: Effective bandwidth approximation versus P_{eb} for a single stream ($B = 800$, $\tau = 0$).

$P_{eb} = 0.001$, the minimum required bandwidth is $c = 761.9$ cells/sec, which is achieved when $\tau = 1$ (FEC corrects only single-bit errors). Since at $P_{eb} = 0.001$ the mean number of bit errors in a cell is $0.423 < 1$, the advantage of correcting multiple-bit errors is overshadowed by the extra FEC bandwidth overhead. Note that the optimal code rate is always achieved at a nonzero τ, implying that resource allocation for a guaranteed CLR can always be improved using a combined ARQ/FEC approach. It can be observed from Figures 15-17 that the optimal code rate increases with P_{eb}. For $P_{eb} = 0.01$ and $P_{eb} = 0.015$, the optimal values of τ are given by $\tau = 7$ and $\tau = 10$, respectively. The optimal code rate depends on the channel BERs and the target CLR. This suggests the need for adaptive FEC to continuously maintain an optimal code rate for a wireless channel with time-varying characteristics.

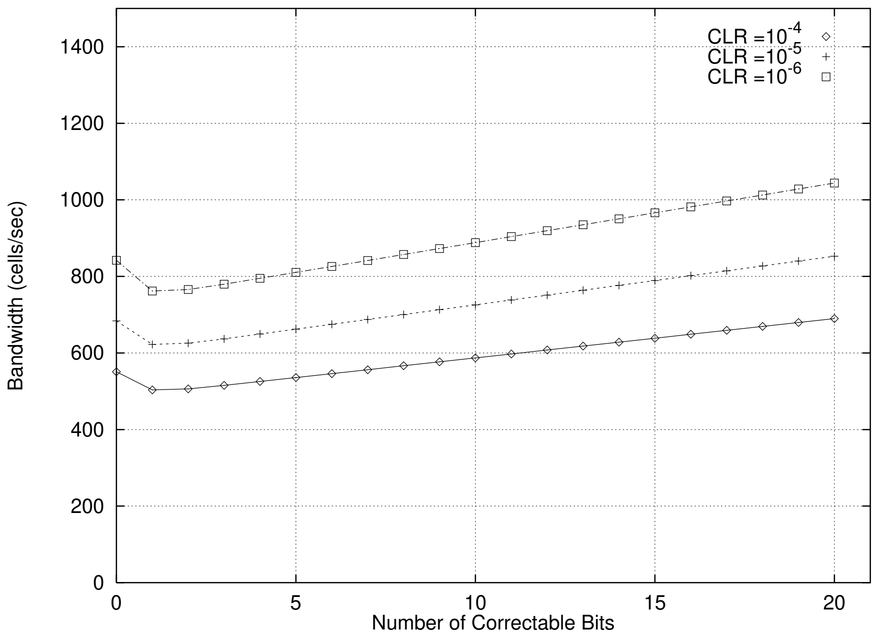

Figure 15: Effective bandwidth versus τ for a single stream ($P_{eb} = 0.001$).

Next, we examine the CLR for multiplexed streams based on the results in Section 5. We consider homogeneous on-off sources with the same target CLR. For brevity, we report the results for ARQ only (i.e., $\tau = 0$). We set $P_{eb} = 10^{-3}$ and $c = 10$ Mbps, and we vary the number of multiplexed streams. To test the goodness of our CLR analysis, which was obtained using the CDE approximation, we compare it to the exact analysis, given in Appendix B. We also present the results based on two other approximations: the asymptotic and Binomial approximations. Both approximations rely on the dominant eigenvalue, similar to the CDE approach. However, they differ from it in the estimation of L; the coefficient associated with the dominant eigenvalue. In the asymptotic approximation, the exact value of L, denoted by L_a, is used, which is obtained from the exact analysis in Appendix B. The Binomial approximation estimates L by L_b, which is

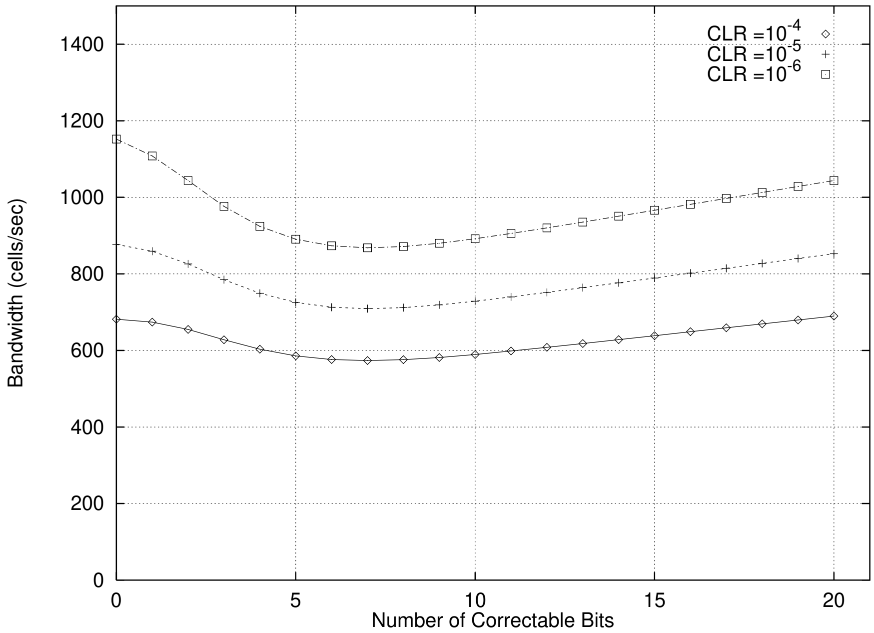

Figure 16: Effective bandwidth versus τ for a single stream ($P_{eb} = 0.01$).

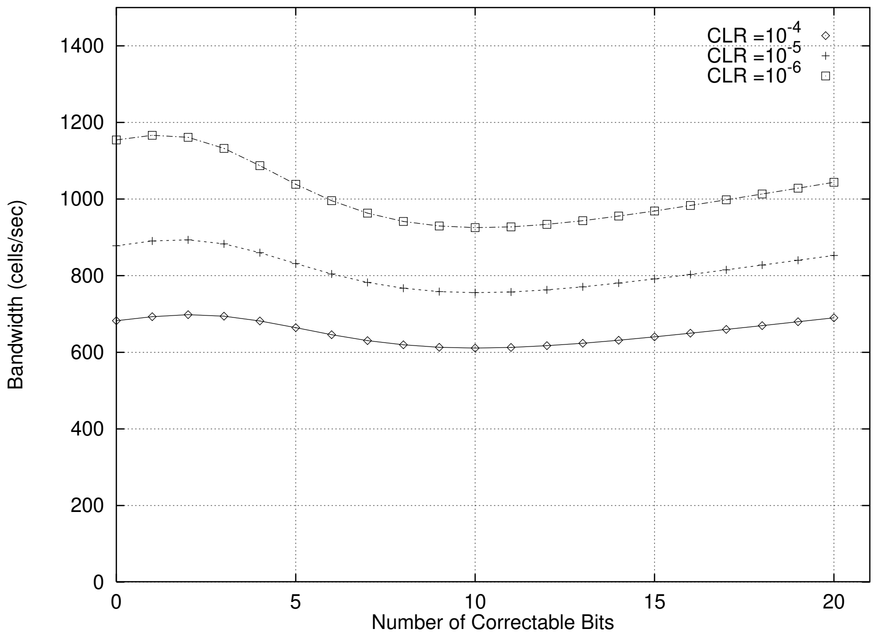

Figure 17: Effective bandwidth versus τ for a single stream ($P_{eb} = 0.015$).

computed from the binomial distribution:

$$L_b \approx G(0) = P[\chi > c] = \sum_{i=j}^{K} \begin{pmatrix} K \\ i \end{pmatrix} w_1^i w_0^{K-i}$$

where $j \triangleq \lceil c/r \rceil$, and w_1 and w_0 are the steady-state probabilities that a source is in on and off states, respectively.

Figures 18, 19, and 20 depict the CLR for 40, 50, and 60 multiplexed connections, respectively, which correspond to traffic loads of 43.6%, 54.5%, and 65.4%. It is observed that the asymptotic approximation is quite accurate compared with the exact result. Thus, it can be argued that one eigenvalue is good enough to compute the CLR for multiplexed streams. As shown in these figures, the difference between the exact results and both the CDE and Binomial approximations tends to decrease as K increases. Both approximations provide upper bounds on the exact CLR, with the Binomial approximation being the tighter of the two. Since in our case only homogeneous on-off sources are considered, the binomial approximation is rather easy to compute. However, if we consider more general sources, it will incur substantial numerical complexity.

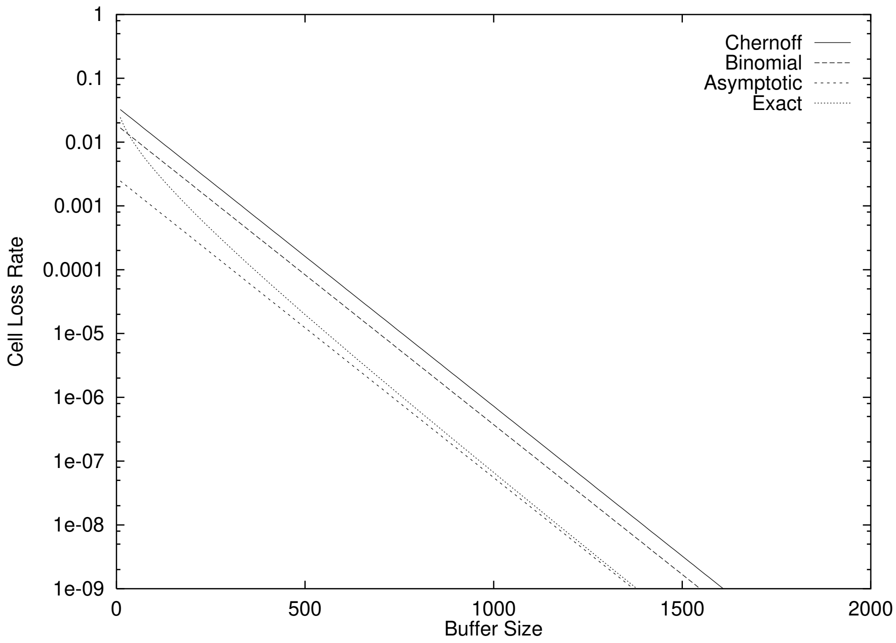

Figure 18: Cell loss rate for 40 multiplexed streams.

The three approximations for the CLR are compared in Table 3. Under light load ($K = 10, 20, 30$), we can see that both the CDE and Binomial approximations deviate largely from the ideal asymptote. Thus, a better approximation for L is still needed when K is relatively small.

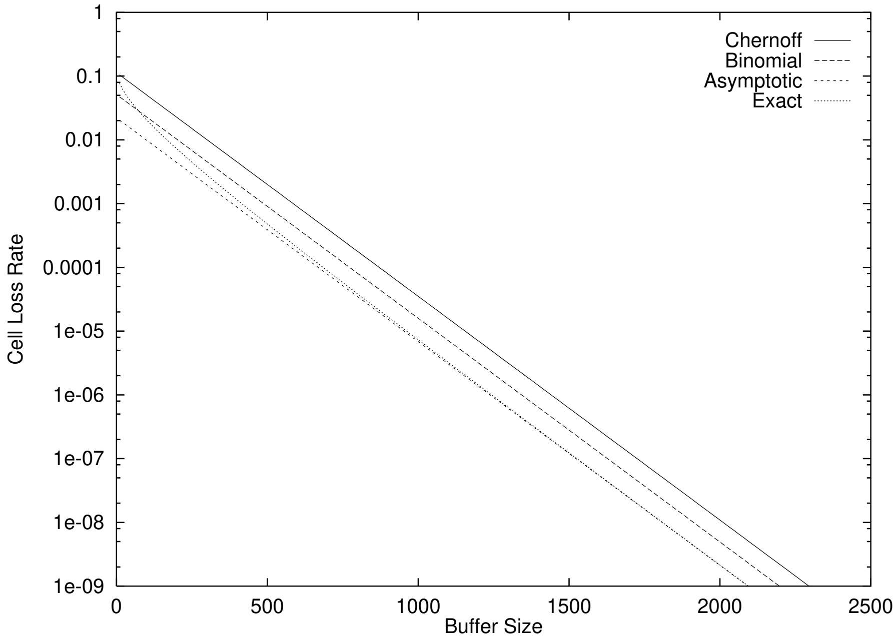

Figure 19: Cell loss rate for 50 multiplexed streams.

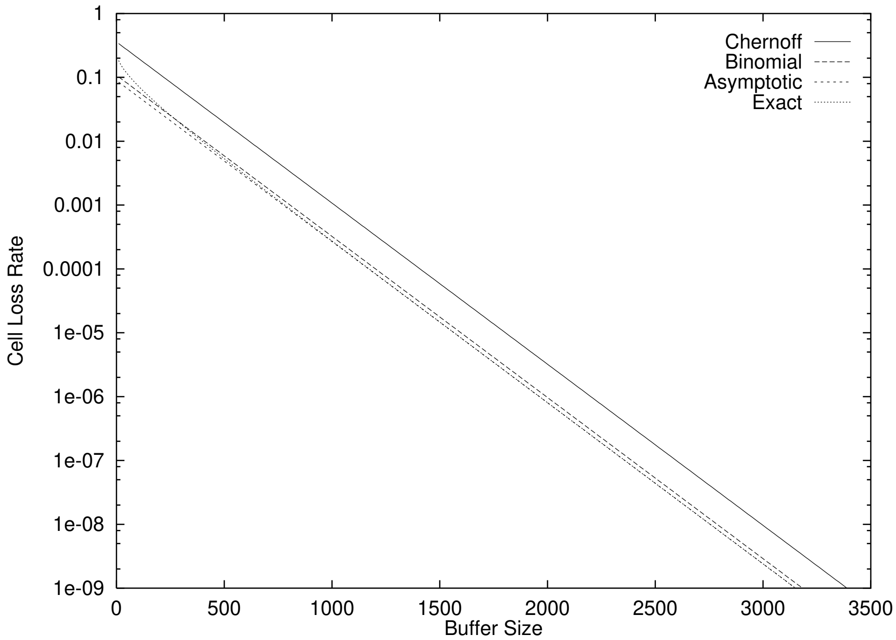

Figure 20: Cell loss rate for 60 multiplexed streams.

K	L_c (CDE)	L_b (Binomial)	L_a (Asymptotic)	L_c/L_a	L_b/L_a
10	4.763×10^{-6}	1.2×10^{-6}	1.151×10^{-8}	413.75	104.31
20	7.667×10^{-4}	3.441×10^{-4}	8.254×10^{-7}	928.92	416.88
30	8.078×10^{-3}	4.169×10^{-3}	1.061×10^{-4}	76.13	39.29
40	0.0361371	0.0185953	0.002747	13.15	6.77
50	0.113547	0.0514114	0.02214	5.13	2.32
60	0.358695	0.107971	0.08951	4.0	1.2

Table 3: The coefficients L_c, L_b, L_a versus the number of multiplexed connections K.

7 Conclusions

In this paper, we investigated the cell loss performance due to buffer overflow at the transmitter side of a wireless ATM link. We used accurate fluid models to capture the bursty nature of ATM traffic. The fluctuations of the wireless channel were appropriately captured using a fluid version of Gilbert-Elliot model. Error control schemes (ARQ and FEC) were incorporated. The cell loss performance was analyzed for a single and for multiplexed sources. In the case of a single stream, the exact CLR was obtained, which only requires the solution of a polynomial of order three. The solution was then used to obtain an approximation for the wireless effective bandwidth, which can be used as a valuable tool in resource allocation and admission control in wireless ATM networks. In the case of multiplexed streams, an approximate expression for the CLR was obtained. Our analytical results were contrasted with simulations of a wireless ATM link with a hybrid ARQ/FEC error control mechanism. We observed that in the case of a single stream (i.e., no multiplexing), the analytical expressions for the CLR and (approximate) wireless effective bandwidth are quite acceptable over a wide range of bit error rates. The approximate CLR for multiplexed streams is adequate under medium and high loads. A better approximation is needed when the load is light. We found that a combined ARQ/FEC is always more efficient (in terms of reducing the per-stream bandwidth requirement) than ARQ alone. The selection of the FEC code rate is very crucial to achieving optimal use of the wireless bandwidth and in the provisioning of QoS over a wireless ATM link. Our focus in this paper was on the cell loss rate, as the primary measure of QoS. In the future, we plan to investigate the delay performance over the wireless ATM link, with an imposed limit on the number of cell retransmissions.

APPENDIX

A Calculation of the Eigenvalues for the Single Stream case

Arranging (25), we obtain

$$az^4 + bz^3 + cz^2 + dz = 0 \tag{53}$$

where

$$
\begin{aligned}
a &= c_g c_b (r - c_g)(r - c_b) && (54) \\
b &= -r^2(c_g\gamma + c_b\delta + c_b\beta + c_g\beta) \\
&\quad -r((c_g + c_b)^2(\beta + \gamma) - c_b^2(\gamma - \delta) + 2c_g c_b(\alpha + \delta)) \\
&\quad -c_g c_b((\alpha + \beta)(c_g + c_b) + 2(\delta c_b + \gamma c_g)) && (55) \\
c &= \alpha^2 c_b c_g + \beta^2 (r - c_b)(r - c_g) \\
&\quad +(c_b\delta + c_g\gamma)(c_b\delta + c_g\gamma - \delta r - \gamma r) \\
&\quad +\beta(c_b^2\delta + 2c_b c_g\delta + 2c_b c_g\gamma \\
&\quad +c_g^2\gamma - 2c_b\delta r - 2c_g\delta r - 2c_b\gamma r - 2c_g\gamma r + \delta r^2 + \gamma r^2) \\
&\quad +\alpha(c_b^2\delta + 2c_b c_g\delta + 2c_b c_g\gamma \\
&\quad +c_g^2\gamma - 2c_b\delta r - 2c_g\gamma r + \beta(2c_b c_g - c_b r - c_g r)) && (56) \\
d &= (\alpha + \beta + \delta + \gamma)(r\beta(\delta + \gamma) - (\alpha + \beta)(c_g\gamma + c_b\delta)). && (57)
\end{aligned}
$$

Eliminating the zero root, the other nonzero eigenvalues are obtained by solving the following equation:

$$z^3 + c_1 x^2 + c_2 x + c_3 = 0$$

where $c_1 = \frac{b}{a}, c_2 = \frac{c}{a}$, and $c_3 = \frac{d}{a}$. If the cubic equation has the three real roots, the roots are given by [20]:

$$
\begin{aligned}
z_1 &= -2\sqrt{Q}\cos\left(\tfrac{\theta}{3}\right) - \tfrac{c_1}{3} \\
z_2 &= -2\sqrt{Q}\cos\left(\tfrac{\theta+2\pi}{3}\right) - \tfrac{c_1}{3} \\
z_3 &= -2\sqrt{Q}\cos\left(\tfrac{\theta-2\pi}{3}\right) - \tfrac{c_1}{3}
\end{aligned}
\tag{58}
$$

where

$$
\begin{aligned}
Q &\triangleq \frac{c_1^2 - 3c_2}{9} \\
R &\triangleq \frac{2c_1^3 - 9c_1c_2 + 27c_3}{54}
\end{aligned}
$$

$$\theta = \arccos(R/\sqrt{Q^3}).$$

B Multiple On-Off Sources over a Wireless Channel

We consider multiple homogeneous on-off sources multiplexed over a wireless channel. The source and channel parameters were given in Section 3. Because of the homogeneity of the sources, the state of the arrival process is indicated by the number of active sources. The infinitesimal generator $\boldsymbol{M}_1$ for this traffic generation process is given by:

$$\boldsymbol{M}_1 = \begin{bmatrix} -K\beta & K\beta & & & & \\ \alpha & -(\alpha+(K-1)\beta) & (K-1)\beta & & & \\ & \vdots & & & \vdots & \\ & & & (K-1)\alpha & -((K-1)\alpha+\beta) & \beta \\ & & & & K\alpha & -K\alpha \end{bmatrix}. \tag{59}$$

In [18] Mitra provided an approach to obtaining the eigenvalues and eigenvectors of the system characterized by (59). Because of the decomposability of the underlying wireless ATM model (as discussed in Section 5), we can apply Mitra's approach and obtain the exact CLR for multiplexed streams. For the cell production part (the arrival process), the adaptation of Mitra's results is rather straightforward, and will be skipped for brevity. In [18] the cell delivery (consumption) part was analyzed assuming that the service rates are multiples of some fixed (basic) rate. In our case, this assumption is no longer applicable, since the two service rates (c_g and c_b, with $c_g > c_b$) can take any values. In the following, we extend Mitra's results on the consumption part to the model in hand.

By equating (4.7ii) in [18] and (23) in terms of zv, we obtain

$$\frac{K}{2}(rz+\alpha+\beta) + \left(k_1 - \frac{K}{2}\right)\sqrt{Q_1(z)} = \frac{z(c_g+c_b)-\delta-\gamma}{2} - \left(k_2 - \frac{1}{2}\right)\sqrt{Q_2(z)}. \tag{60}$$

Rearranging the above equation and squaring both sides, we obtain

$$\begin{aligned} P(z,k_1,k_2) \quad &\triangleq \quad \left(\left(k_1 - \frac{K}{2}\right)^2 Q_1(z) + \left(k_2 - \frac{n}{2}\right)^2 Q_2(z) - L^2(z)\right)^2 \\ &-4\left(k_1 - \frac{K}{2}\right)^2 \left(k_2 - \frac{n}{2}\right)^2 Q_1(z)Q_2(z) = 0 \end{aligned} \tag{61}$$

where

$$L(z) \triangleq \frac{K}{2}(rz+\alpha+\beta) - \frac{z(c_g+c_b)-\delta-\gamma}{2} \tag{62}$$

and $Q_1(z)$ and $Q_2(z)$ are given in (21) and (24). Equation (61) is valid for k_1 and k_2 in the set $\{0, 1, \ldots, K-1\}$. For given values of k_1 and k_2, (61) is a polynomial or order four, with a maximum of four real roots. Mitra showed that in order to obtain unique real roots, (61) needs only to be solved for $0 \leq k_1 \leq K/2$ and $0 \leq k_2 \leq 1$. Therefore, the required eigenvalues are the real-valued solutions of the polynomials $P(z, k_1, k_2) = 0$, $0 \leq k_1 \leq K/2$ and $0 \leq k_2 \leq 1$.

So far, we have discussed how to obtain the eigenvalues. The eigenvector $\boldsymbol{\phi}_1$ can be obtained by using Equation (5.7) in [18]. The eigenvectors $\boldsymbol{\phi}_2$ for the cell delivery part are given in (27). Thus, the resulting eigenvectors $\boldsymbol{\phi}$ are obtained by the following Equation:

$$\boldsymbol{\phi} = \boldsymbol{\phi}_1 \otimes \boldsymbol{\phi}_2.$$

Finally, the stationary buffer content distribution $\boldsymbol{\Pi}(x)$ is given by:

$$\boldsymbol{\Pi}(x) = a_d \boldsymbol{w} + \sum_{z_i < 0} a_i \exp(z_i x) \boldsymbol{\phi}_i \tag{63}$$

where $\boldsymbol{w} = \boldsymbol{w}_1 \otimes \boldsymbol{w}_2$, $\boldsymbol{w}_1$ is given in (2.18) in [18], and $\boldsymbol{w}_2$ is given by

$$\boldsymbol{w}_2 = \begin{bmatrix} \frac{\gamma}{\delta+\gamma} & \frac{\delta}{\delta+\gamma} \end{bmatrix}.$$

In order to calculate the coefficients a_i, we use the boundary conditions:

$$\begin{aligned} \Pi_s(0) &= 0, \quad \text{for } z_i < 0, \text{with } \chi_i > c_g \text{ or } \chi_i > c_b \\ a_d &= 1, \quad (\text{since } \boldsymbol{\Pi}(\infty) = \boldsymbol{w}) \end{aligned}$$

where χ_i denote the total source rate associated with the eigenvalue z_i. The cell loss rate is then obtained using (32).

References

[1] A. S. Acampora and M. Naghshineh, “An architecture and methodology for mobile–executed handoff in cellular ATM networks,” *IEEE J. Select. Areas Commun.*, vol. 12, no. 8, pp. 1365–1375, Oct. 1994.

[2] A. Acampora, “Wireless ATM: a perspective on issues and prospects,” *IEEE Pers. Commun.*, vol. 3, no. 4, pp. 8–17, Aug. 1996.

[3] E. Ayanoglu, K. Y. Eng, and M. J. Karol, “Wireless ATM: limits, challenges, and protocols,” *IEEE Pers. Commun.*, vol. 3, no. 4, pp. 18–34, 1996.

[4] D. Anick, D. Mitra, and M. M. Sondhi, “Stochastic theory of a data–handling system with multiple sources,” *Bell Syst. Tech. J.*, vol. 61, pp. 1871–1894, 1982.

[5] H. Balakrishnan, V. N. Padmanabhan, S. Seshan, and R. H. Katz, “A comparison of mechanisms for improving TCP performance over wireless links,” *IEEE/ACM Trans. Networking*, vol. 5, no. 6, pp. 756–769, Dec. 1997.

[6] J. B. Cain and D. N. McGregor, “A recommended error control architecture for ATM networks with wireless links,” *IEEE J. Select. Areas Commun.*, vol. 15, no. 1, pp. 16–28, Jan. 1997.

[7] G. L. Choudhury, D. M. Lucatoni, and W. Whitt, “Squeezing the most out of ATM,” *IEEE Trans. Commun.*, vol. 44, no. 2, pp. 203–217, Feb. 1996.

[8] A. I. Elwalid and D. Mitra, “Effective bandwidth of general Markovian traffic sources and admission control of high speed networks,” *IEEE/ACM Trans. Networking*, vol. 1, no. 3, pp. 329–343, Jun. 1993.

[9] A. Elwalid, D. Heyman, T. V. Lakshman, D. Mitra, and A. Weiss, “Fundamental bounds and approximations for ATM multiplexers with applications to video teleconferencing,” *IEEE J. Select. Areas Commun.*, vol. 13, no. 6, pp. 1004–1016, Aug. 1995.

[10] R. Fantacci, “Queueing analysis of the selective repeat automatic repeat request protocol wireless packet networks,” *IEEE Trans. Veh. Technol.*, vol. 45, no. 2, pp. 258–264, May 1996.

[11] R. J. Gibbens and P. J. Hunt, “Effective bandwidths for the multi-type UAS channel,” *Queueing Syst.*, vol. 9, pp. 17–28, 1991.

[12] R. Guérin, H. Ahmadi, and M. Naghshineh, “Equivalent capacity and its application to bandwidth allocation in high–speed networks,” *IEEE J. Select. Areas Commun.*, vol. 9, no. 7, pp. 968–981, Sep. 1991.

[13] N. Guo and S. D. Morgera, "Frequency-hopped ARQ for wireless network data services," *IEEE J. Select. Areas Commun.*, vol. 12, no. 8, pp. 1324–1336, Sep. 1994.

[14] I. Joe and I. F. Akyildiz, "An adaptive hybrid ARQ scheme with concatenated FEC codes for wireless ATM," *Proc. MobiCom '97*, pp. 131–138, Sep. 1997.

[15] F. P. Kelly, "Effective bandwidths at multi-type queues," *Queueing Syst.*, vol. 9, pp. 5–15, 1991.

[16] S. Lin and D. J. Costello, Jr., *Error Control Coding: Fundamentals and Applications*, Englewood Cliffs, NJ: Prentice-Hall, 1983.

[17] H. Liu and M. El Zarki, "Performance of H.263 video transmission over wireless channels using hybrid ARQ," *IEEE J. Select. Areas Commun.*, vol. 15, no. 9, pp. 1775–1786, Dec. 1997.

[18] D. Mitra, "Stochastic theory of a fluid model of producers and consumers coupled by a buffer,"*Adv. Appl. Prob.*, vol. 20, pp. 646–676, 1988.

[19] A. Mohammadi, S. Kumar, and D. Klynmyshyn, "Characterization of effective bandwidth as a metric of quality of service for wired and wireless ATM networks," in *Proc. IEEE ICC*, vol. 2, pp. 1019–1024, 1997.

[20] W. H. Press, S. A. Teukolsky, W. T. Vetterling, and B. P. Flannery, *Numerical Recipes in C*, 2nd ed. Cambridge University Press, 1992.

[21] D. Raychaudhuri and N. D. Wilson, "ATM-based transport architecture for multiservices wireless personal communication networks," *IEEE J. Select. Areas Commun.*, vol. 12, no. 8, pp. 1401–1414, Oct. 1994.

[22] M. Rice and S. B. Wicker, "Adaptive error control for slowly varying channels," *IEEE Trans. Commun.*, vol. 42, no. 2/3/4, pp. 917–925, Feb./Mar./Apr. 1994.

[23] T. Sato, M. Kawabe, T. Kato, and A. Fukasawa, "Throughput analysis method for hybrid ARQ schemes over burst error channels," *IEEE Trans. Veh. Technol.*, vol. 42, no. 1, pp. 110–117, Feb 1993.

[24] M. Zukerman, P. L. Hiew, and M. Gitlits, "FEC code rate and bandwidth optimization in WATM networks," *Multiaccess, Mobility, and Teletraffic: Advances in Wireless Networks*, D. Everitt and M. Rumsewicz, Eds., pp. 207–220, Boston: Kluwer, 1998.